# Gelsolin-Like Domain 3 Plays Vital Roles in Regulating the Activities of the Lily Villin/Gelsolin/Fragmin Superfamily

Dong Qian[1☯], Qiong Nan[1☯], Yueming Yang[1], Hui Li[1], Yuelong Zhou[1], Jingen Zhu[1], Qifeng Bai[2], Pan Zhang[1], Lizhe An[1], Yun Xiang[1] *

1 MOE Key Laboratory of Cell Activities and Stress Adaptations, School of Life Sciences, Lanzhou University, Lanzhou, 730000, China, 2 College of Chemistry and Chemical Engineering, Lanzhou University, Lanzhou, 730000, China

☯ These authors contributed equally to this work.
* xiangy@lzu.edu.cn

## Abstract

The villin/gelsolin/fragmin superfamily is a major group of $Ca^{2+}$-dependent actin-binding proteins (ABPs) involved in various cellular processes. Members of this superfamily typically possess three or six tandem gelsolin-like (G) domains, and each domain plays a distinct role in actin filament dynamics. Although the activities of most G domains have been characterized, the biochemical function of the G3 domain remains poorly understood. In this study, we carefully compared the detailed biochemical activities of ABP29 (a new member of this family that contains the G1-G2 domains of lily ABP135) and $ABP135_{G1-G3}$ (which contains the G1-G3 domains of lily ABP135). In the presence of high $Ca^{2+}$ levels in vitro (200 and 10 μM), $ABP135_{G1-G3}$ exhibited greater actin severing and/or depolymerization and nucleating activities than ABP29, and these proteins had similar actin capping activities. However, in the presence of low levels of $Ca^{2+}$ (41 nM), $ABP135_{G1-G3}$ had a weaker capping activity than ABP29. In addition, ABP29 inhibited F-actin depolymerization, as shown by dilution-mediated depolymerization assay, differing from the typical superfamily proteins. In contrast, $ABP135_{G1-G3}$ accelerated F-actin depolymerization. All of these results demonstrate that the G3 domain plays specific roles in regulating the activities of the lily villin/gelsolin/fragmin superfamily proteins.

## Introduction

The villin/gelsolin/fragmin superfamily is an important class of multifunctional actin-binding proteins (ABPs) that regulate dynamic remodeling of the actin cytoskeleton via actin nucleating, severing, capping and bundling activities in eukaryotes [1–3]. These superfamily proteins are typified by the possession of three or six G domains [1,4,5]. In mammals and bacteria, each member of this superfamily is encoded by distinct genes, such as villin, which contains six G domains and one head piece domain [6,7]; gelsolin, which contains six G domains [1,4];

fragmin/severin, which has three G domains [8]; and GSNL-1 in *Caenorhabditis elegans*, which contains four G domains [9]. However, although the genes encoding villin have been reported in detail[10–12], gelsolin-like proteins in plants have only been mentioned in a few reports [12,13]. The first two plant villins to be identified were ABP135 [14,15] and ABP115 [16,17], which were isolated from lily pollen. In addition, there are six villin homologs in *Oryza sativa* and five in *Arabidopsis thaliana* [10,18]. Recently, two new members were identified: PrABP80 [13], which was isolated from *poppy* pollen and contains six G domains, and LdABP41 [19], which was isolated from *Lilium davidii* pollen and contains the G1-G3 domains. Interestingly, the smallest identified member of the superfamily is ABP29 [20], which contains only the G1 and G2 domains and part of the G2-G3 linker from *Lilium* pollen and is an alternative splicing product of plant ABP135 [20,21].

Despite sharing conserved protein sequences and three-dimensional structures, each G domain of the villin/gelsolin/fragmin superfamily plays a distinct role in actin dynamics, endowing the proteins with multifunctional and distinct activities [1,12]. Through several decades of research, the biochemical functions of most G domains in this superfamily have been well characterized. For example, the N-terminal 17-kD chymotryptic segment (CT14N) that retains weak actin-binding functions was described as the G1 domain, which can bind to monomeric actin in a $Ca^{2+}$-insensitive manner [22]. The truncation of gelsolin with G1 domain and 10 extra amino acids from the start of the G2 domain has weak F-actin severing activity, but this severing activity of the truncation is only one percent of the full gelsolin protein [23]. The G2 domain contains an F-actin binding site, which also has actin capping activity [24]. In addition, the G2 domain has a phosphatidylinositol 4,5-bisphosphate ($PIP_2$) binding site and binds to tropomyosin in a $Ca^{2+}$- and pH-sensitive manner [24,25]. Further, the G2 domain of GSNL-1 functions as a regulatory domain for $Ca^{2+}$-dependent conformational changes [26]. Similar to the G1 domain, the G4 domain also binds to monomeric actin [5,27] In addition, it is generally accepted that the C-terminus of gelsolin acts as a helix latch and binds the G2 domain to maintain gelsolin in a $Ca^{2+}$-free compact state [5,28,29]. However, the biochemical function of the G3 domain is still poorly understood beyond its role as a spacer.

We have previously demonstrated that both ABP29 and LdABP41 accelerate actin nucleation, severing and capping of actin filaments in a $Ca^{2+}$- and/or $PIP_2$-regulated manner *in vitro* [19,20,30]. Surprisingly, significant differences between ABP29 and LdABP41 and other gelsolin-like proteins have been shown in dilution-mediated F-actin depolymerization assays [20,30]. Specifically, ABP29 inhibits F-actin depolymerization, whereas LdABP41 accelerates F-actin depolymerization similar to other typical members of this superfamily. Why is this? Does the loss of the G3 domain cause this difference? Unfortunately, the gene encoding LdABP41 has not been cloned, although mass spectrometry analysis has shown that LdABP41 shares substantial similarity with lily ABP135 and that it may possess the full G1-G3 domains [19,30]. Thus, it remains unclear whether LdABP41 contains a complete G3 domain and whether the G3 domain causes the observed difference between ABP29 and LdABP41.

Here, we cloned the G1-G3 domains of ABP135 (and designated them as $ABP135_{G1-G3}$), which behaves similarly to LdABP41 [19,30] *in vitro*. We then carefully compared the activities of ABP29 and $ABP135_{G1-G3}$ in regulating actin dynamics. Our results demonstrated that the G3 domain endows $ABP135_{G1-G3}$ with greater actin severing and/or depolymerization and nucleating abilities than ABP29 in the presence of high $Ca^{2+}$ but that its actin capping activity is weaker than that of ABP29 in the presence of low $Ca^{2+}$. These findings shed new light on the functions of the G3 domain.

**Table 1. Primers used in this study.**

| Primer name | Sequence (5'–3') |
| --- | --- |
| ABP135$_{G1-G3}$-F | GAATTCATGGCCAACTCTTCAAAAAT |
| ABP135$_{G1-G3}$-R | GTCGACAGACTCAAAGTTGGACTTAAA |
| ABP29-F | GAATTCATGGCCAACTCTTCAAAAAT |
| ABP29-G1-2-R | GTCGACTCAACCTGACCCAGATTCTGCTG |
| ABP29-linker-R | GTCGACTCAATAAAGCTTCCCTGGCGTGG |

The restriction enzyme sites are underlined.

"(F)" indicates the forward primer and

"(R)" indicates the reverse primer.

## Materials and Methods

### Expression and purification of recombinant proteins

The cDNA coding sequence (CDS) of ABP135$_{G1-G3}$ was amplified from lily flowers, and ABP29$_{G1-G2}$ and ABP29-△C6 were amplified from pGEX-4T-ABP29 [20]. The primers used for cloning are described in the Table 1. To obtain recombinant proteins, ABP135$_{G1-G3}$, ABP29$_{G1-G2}$ and ABP29-△C6 were cloned into the pGEX-4T vector and then expressed in the *E. coli* BL21 (DE3) strain by induction with 0.5 mM isopropylthio-β-D-galactopyranoside (IPTG) overnight at 26°C according to previously described methods [31]. Next, recombinant proteins were then affinity-purified using glutathione–Sepharose 4B resin (GE Healthcare) according to the manufacturer's instructions. The purified proteins were dialyzed against modified buffer A3 (10 mM Tris-HCl, 7 mM PIPES, 200 μM CaCl$_2$, 0.5 mM DTT and 0.2 mM ATP, pH 7.0).

According to previously described methods [32,33], actin was isolated from rabbit skeletal muscle acetone powder and labeled on Cys$^{374}$ with pyrene iodoacetamide. Human recombinant profilin I was purified as described previously [34]. Prior to all experiments, all recombinant proteins were preclarified by centrifugation at 100,000 g for 1 h at 4°C.

### High-speed co-sedimentation assay

A high-speed co-sedimentation assay was performed as described by Xiang et al. [20]. Preformed F-actin (5 μM) was incubated with different concentrations of recombinant proteins in the presence of various concentrations of free Ca$^{2+}$ at 22°C for 1 h. The free Ca$^{2+}$ concentration was calculated with EGTA software by Petesmif (http://pcwww.liv.ac.uk/~petesmif/petesmif/software/webware06/EGTA/EGTA.htm), as described in Khurana et al. [35]. According to our calculations, 2 mM, 1 mM, 0.5 mM and 0.2 mM EGTA were equivalent to the volumes of 0.041 μM, 0.091 μM, 0.243 μM and 10 μM free Ca$^{2+}$, respectively, in all of our experimental systems. The samples were centrifuged at 100,000 g for 1 h at 4°C (CS120GXII, Hitachi). Fractions containing the supernatants and pellets were resolved using SDS-PAGE, and the gels were stained with Coomassie Brilliant Blue R 250. The amounts of actin in the supernatants and pellets were analyzed using Quantity One software (version 4.6.2; Bio-Rad).

### Direct observation of actin filaments by fluorescence microscopy

Microscopic observation of actin filament severing was performed as described previously [20,36]. Preformed F-actin (5 μM) was incubated with 100 or 200 nM ABP29 or ABP135$_{G1-G3}$ in the presence of various concentrations of free Ca$^{2+}$ at room temperature for 30 min, and the

reaction mixtures were labeled with Alexa 488-phalloidin (Molecular Probes Invitrogen), as previously described [6]. Then, the reaction mixtures were diluted to 60 nM with F buffer (10x F buffer: 500 mM KCl, 10 mM MgCl$_2$, 10 mM Tris-HCl, 200 µM CaCl$_2$ and 100 mM ATP, pH 7.0) and 1 µl of each diluted sample was placed on a nitrocellulose-coated coverslip. The samples were observed using a confocal laser-scanning microscope (Olympus FV-300) mounted on a fluorescence microscope (Olympus IX-70) with a 100x oil-immersion objective, and the images were captured using Olympus Fluoview 4.0 software and processed with Adobe Photoshop CS2. Filament lengths were measured using Image J software.

## Actin filament severing assay

An actin filament severing assay was performed as described previously [37] with modifications as follows: 2 µM CapG-actin (1:200) filaments were generated by polymerization overnight at 25°C in S2 buffer (0.5 mM ATP, 1 mM DTT, 200 µM CaCl$_2$, 0.1 mM KCl, 1 mM MgCl$_2$, and 10 mM Tris-HCl, pH 7.5) with 5% pyrene-labeled actin and CapG (purified from recombinant protein expressed in *E. coli* BL21). Then, the addition of S2 buffer diluted actin filaments to 100 nM with varying concentrations of ABP29 or ABP135$_{G1-G3}$, and immediately the decrease in pyrene fluorescence intensity that accompanied actin depolymerization was monitored for 300 s.

## Actin nucleation assay

Actin nucleation was performed as described previously [20]. Monomeric actin (5 µM 5% pyrene-labeled) was incubated with various concentrations of ABP29 or ABP135$_{G1-G3}$ at room temperature for 5 min in the presence of 200 µM, 10 µM or 0.041 µM free Ca$^{2+}$. Pyrene fluorescence was monitored for 100 s with a Fluoro-Max-4$^{®}$ spectrofluorometer (HORIBA Jobin Yvon) immediately after the addition of one-tenth volume of 10x F buffer.

## Actin filament elongation assay

An elongation assay was performed as described previously [20,38]. Prepared actin filament seeds (0.4 µM) were incubated with different concentrations of ABP29 or ABP135$_{G1-G3}$ in the presence of different Ca$^{2+}$ concentrations at room temperature for 5 min and then supplemented with 1 µM G-actin (5% pyrene-labeled) saturated with 4 µM human profilin I and one-tenth volume of 10x F buffer. After actin elongation was initiated, the change in pyrene fluorescence accompanying actin polymerization was monitored.

## Critical concentration determination

According to a previously described method [9], pyrene-labeled G-actin (5% labeled) at varying concentrations (0–4 µM) was polymerized for 18 h at room temperature in the presence of 0.5 µM ABP29 or ABP135$_{G1-G3}$ in F buffer, and the final fluorescence intensity of pyrene (excitation at 365nm and emission at 407 nm) was measured.

## Actin filament depolymerization assay

Dilution assays were performed according to a previously described method [20]. Briefly, various concentrations of the recombinant proteins were incubated with 5 µM preformed F-actin (50% pyrene-labeled) in the presence of different concentrations of free Ca$^{2+}$ for 5 min at room temperature. The decrease in pyrene fluorescence intensity that accompanied actin depolymerization was monitored for 400 s after the solution was diluted 25-fold with G buffer (5 mM Tris-HCl, 0.2 mM ATP and 0.5 mM DTT, pH 8.0) containing various concentrations of CaCl$_2$.

## Statistical analysis

Statistical analyses were conducted using SPSS 16.0 followed by Student's $t$ test. At least three independent experiments were performed.

## Accession numbers

The sequence data from this article can be found in the GenBank/EMBL databases under the following accession numbers: ABP29 (EF042093), ABP135 (AAD54660), Human cap G (NP_001243068.1) and Human Gelsolin (NM_198252).

## Results

### The actin severing and/or depolymerization activity of ABP135$_{G1-G3}$ is stronger than that of ABP29 in the presence of high concentrations of calcium

To identify whether the G3 domain has an effect on the activities of villin/gelsolin/fragmin superfamily members, we generated different truncated variants of lily ABP135 and ABP29 using deletion mutagenesis (Fig 1A). Initially, we purified recombinant GST-ABP29 and GST-ABP135$_{G1-G3}$ (0–342 AA) to test the function of the G3 domain in F-actin severing and/or depolymerization (Fig 1B). According to previous studies, the growing pollen tube possesses a "tip-focused" gradient of free $Ca^{2+}$, in which the cytosolic concentration of free $Ca^{2+}$ ranges from 2–10 μM (in the apical region) to 20–200 nM (in the shank region) [39–41]; therefore, we selected $Ca^{2+}$ concentrations for our experiments that corresponded to *in vivo* function. The specific protein concentrations for our experiments were chosen based on previous work [19,20,30]. A high-speed co-sedimentation assay was performed in the presence of 0.3, 0.6 and 1 μM ABP29 or ABP135$_{G1-G3}$. In the presence of 200 μM $Ca^{2+}$, the presence of ABP29 or ABP135$_{G1-G3}$ caused a significant amount of actin to be redistributed to the supernatant in a dose-dependent manner (Fig 1C–1F), in agreement with our previous studies [19,20]. In addition, in the presence of high concentrations of $Ca^{2+}$ (200 μM and 10 μM), ABP135$_{G1-G3}$ increased the amount of supernatant actin to a greater degree than ABP29 did. In the presence of low concentrations of $Ca^{2+}$, such as 243 nM, 91 nM and 41 nM, there were no obvious differences in the amounts of supernatant actin between the two proteins (Fig 1C, 1D and 1E).

To further confirm the above results, fluorescence microscopy was employed to directly visualize Alexa 488–phalloidin-labeled actin filaments (Fig 2). As shown in Fig 2A, compared with actin alone (average lengths = 9.75 ± 1.94 μm), 100 nM and 200 nM ABP29 significantly reduced the lengths of actin filaments (average lengths = 4.05 ± 0.94 μm and 2.81 ± 0.83 μm, respectively), and 100 nM and 200 nM ABP135$_{G1-G3}$ resulted in even shorter actin filaments (average lengths = 2.23 ± 0.83 μm and 1.05 ± 0.34 μm, respectively). These results indicate that ABP135$_{G1-G3}$ possesses stronger severing and/or depolymerization activity than ABP29 in the presence of 200 μM free $Ca^{2+}$ (Fig 2A). Furthermore, the F-actin severing and/or depolymerization activities of ABP29 and ABP135$_{G1-G3}$ were observed when the $Ca^{2+}$ concentration was changed using EGTA (Fig 2B and 2C). In the presence of 200 μM and 10 μM free $Ca^{2+}$, ABP135$_{G1-G3}$ caused greater amounts of smaller fragmentation of actin filaments compared with ABP29. However, when $Ca^{2+}$ was chelated by EGTA, resulting in a reduction in the concentration (for example, 0.243, 0.091 or 0.041 μM), there was no significant difference in actin filament length between ABP29 and ABP135$_{G1-G3}$, which is consistent with the co-sedimentation assay results described above.

According to the previous work by Xiang et al. (2007), the severing activity of ABP29 was determined by a time course of actin filament fragmentation [20]. To determine whether the
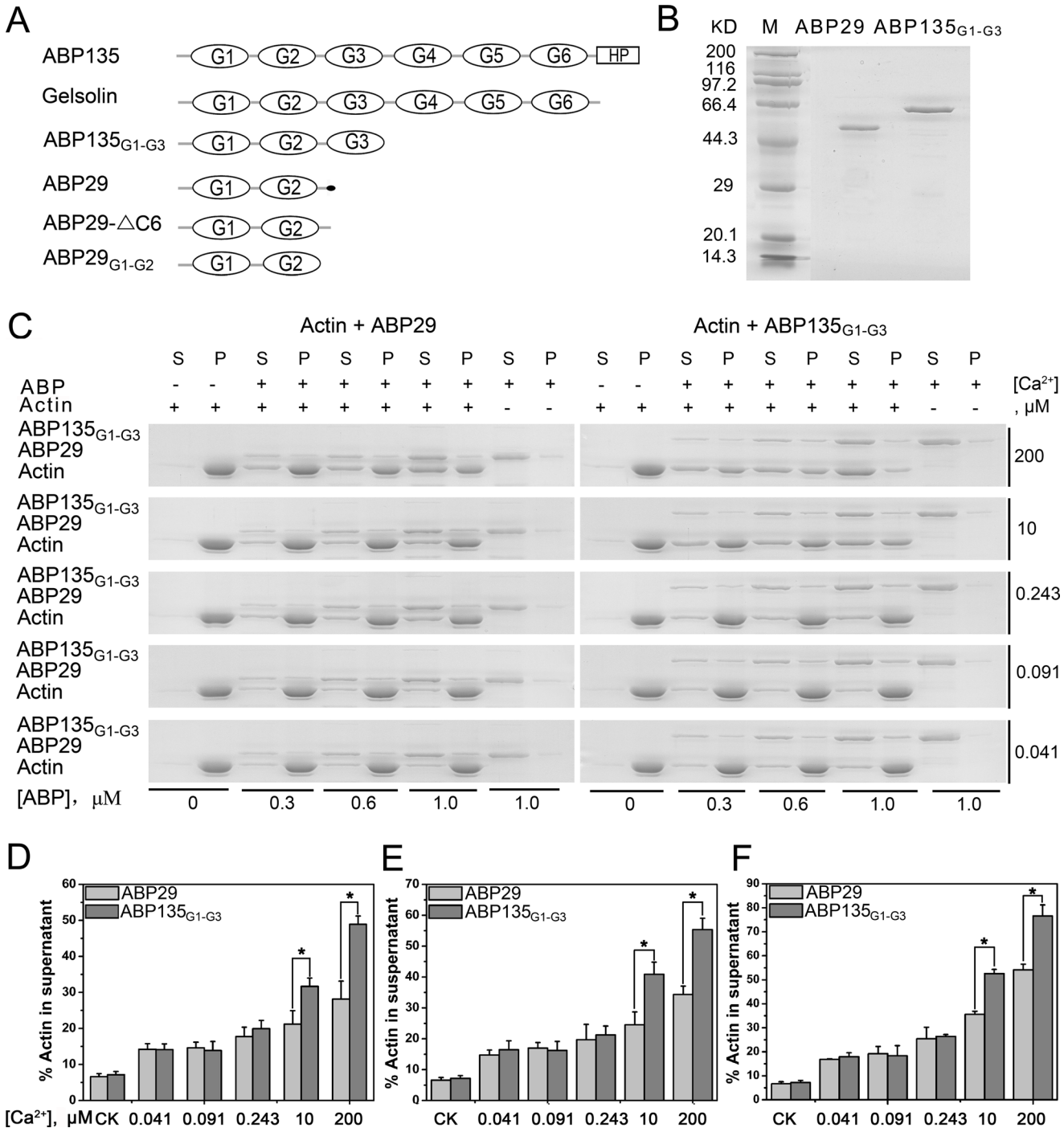
Fig 1. Recombinant ABP29 and ABP135$_{G1-G3}$ fusion proteins sever and/or depolymerize actin filaments in a calcium-dependent manner. (A) Domain structures of gelsolin superfamily members studied in the paper. The lily ABP135,with six G domains and a headpiece (HP) domain at the C-terminus, is designated as ABP135. Full-length human gelsolin, containing six G-domains, is designated as Gelsolin. ABP135$_{G1-G3}$ containing the G1-G3 domains is part of ABP135. *Lilium* ABP29 is a splicing product of ABP135, and the small black dot at the end of ABP29 represents the six amino acids that differ from ABP135. ABP29-△C6 has six fewer amino acids than ABP29 at the C-terminus. ABP29$_{G1-G2}$ contains only the G1-G2 domains of ABP29. (B) SDS-PAGE analysis of purified recombinant ABP29 and ABP135$_{G1-G3}$. Molecular mass markers (M) in kiloDaltons are shown to the left of the gel. (C) Detailed comparison of ABP29 and ABP135$_{G1-G3}$ severing and/or depolymerization activities in the presence of different concentrations of Ca$^{2+}$ with high-speed co-sedimentation assays; "(s)" indicates supernatant, "(p)" indicates pellets, and "ABP" indicates ABP29 or ABP135$_{G1-G3}$. (D-F) Statistical analysis results from (C). The graph shows the percentage of actin in the supernatant. The concentrations of the recombinant proteins are 0.3, 0.6 and 1.0 μM, respectively in (D-F). The CK is the percentage of actin in the supernatant in the absence of ABP. The error bars represent ± SE (n = 3); *P < 0.05 (Student's *t* test).
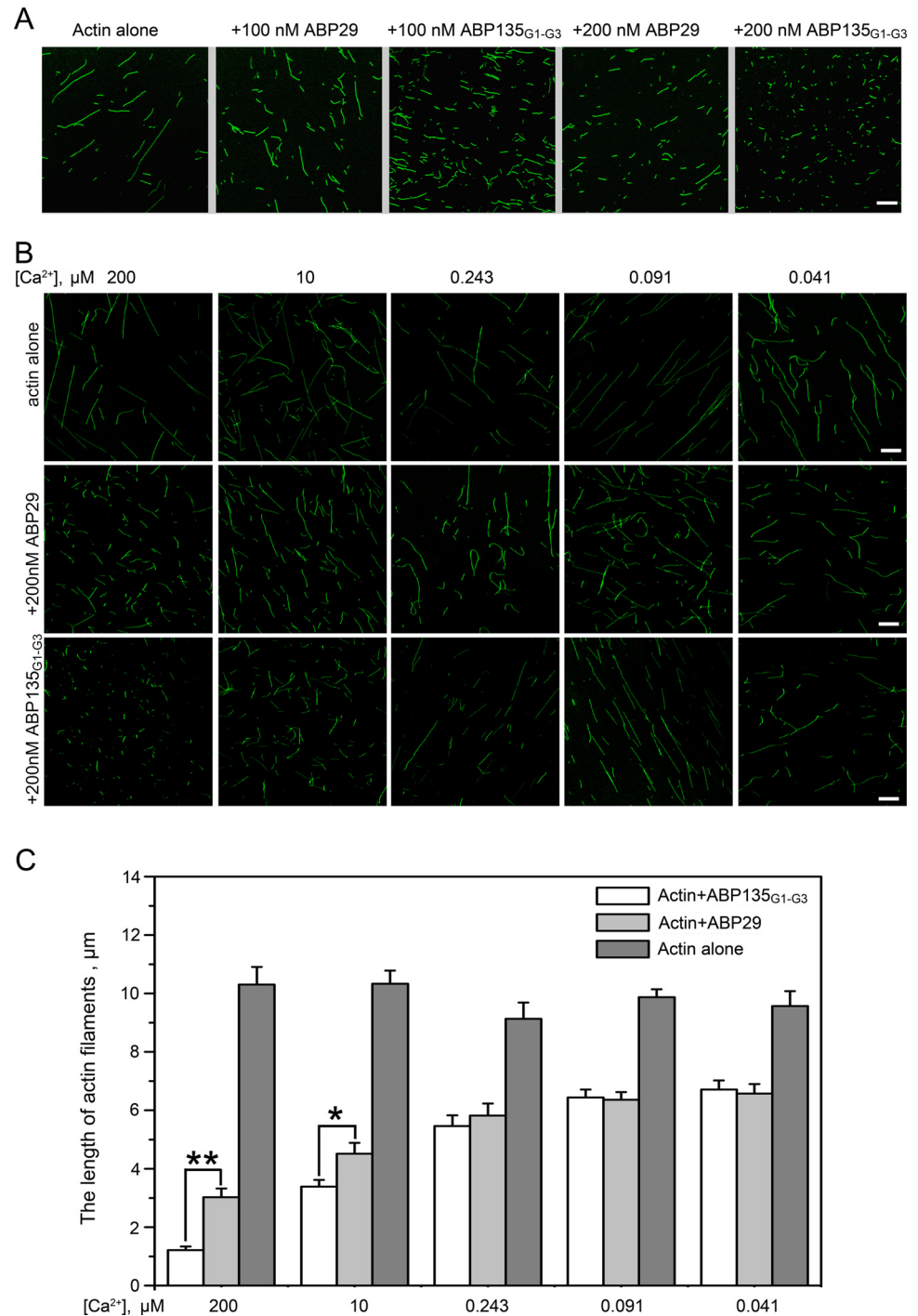
Fig 2. Direct visualization of actin filament severing and/or depolymerization by recombinant ABP29 and ABP135$_{G1-G3}$. (A) Direct observation of the severing and/or depolymerization activities of ABP29 and ABP135$_{G1-G3}$ at different concentrations (100, 200 nM) in the presence of 200 µM free Ca$^{2+}$. The scale bar is 10 µm. (B) Direct observation of the severing and/or depolymerization activities of 200 nM ABP29 and ABP135$_{G1-G3}$ in the presence of various concentrations (200, 10, 0.243, 0.091 and 0.041 µM) of free Ca$^{2+}$. The scale bar is 10 µm. (C) Quantification of actin filament length from the micrographs from (B). The lengths of actin filaments were measured by Image J. Thirty pictures for each condition were analyzed (25–70 actin filaments in every picture), and quantification of 10 pictures represents a single result. Error bars represent ± SE (n = 3). *P < 0.05, **P < 0.01 (Student's t test).
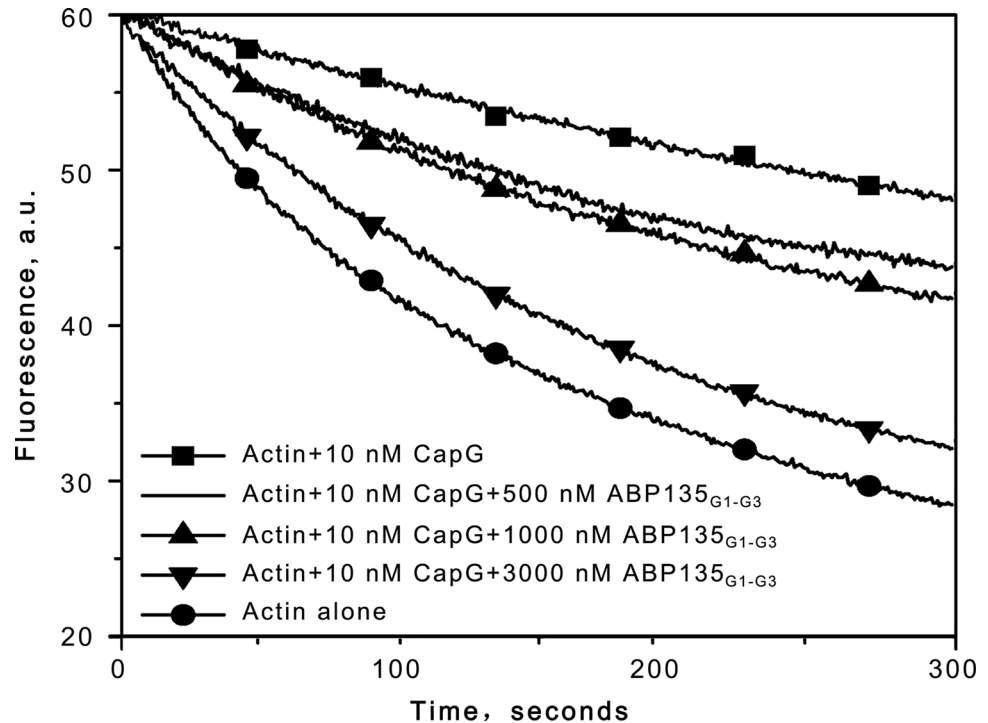
doi:10.1371/journal.pone.0143174.g002

**Fig 3. Effects of ABP135$_{G1-G3}$ on actin filament severing.** A total of 2 µM preformed CapG capped pyrene actin filaments was diluted to 100 nM in S2 buffer with various concentrations of ABP135$_{G1-G3}$, and immediately, the decrease in pyrene fluorescence intensity that accompanied actin depolymerization was monitored for 300 s.

severing by ABP135$_{G1-G3}$ truly takes place, an actin filament severing assay was performed. As shown in Fig 3, ABP135$_{G1-G3}$ severed actin filaments. Collectively, these results demonstrate that the existence of the G3 domain confers ABP135$_{G1-G3}$ with greater F-actin severing and/or depolymerization ability in the presence of high concentrations of $Ca^{2+}$.

## ABP135$_{G1-G3}$ exhibits more effective actin nucleating activity than ABP29 in the presence of high levels of $Ca^{2+}$

To test the effect of the G3 domain on actin polymerization dynamics, pyrene fluorescence was used to monitor rabbit muscle actin polymerization kinetics (Fig 4). Both ABP29 and ABP135$_{G1-G3}$ diminished the lag period corresponding to the nucleation step for actin polymerization in a concentration-dependent manner in the presence of 200 µM or 10 µM free $Ca^{2+}$ (Fig 4A and 4B), but the activity of ABP135$_{G1-G3}$ was higher than that of ABP29. However, when $Ca^{2+}$ was chelated by EGTA, the nucleation activities of ABP29 and ABP135$_{G1-G3}$ were significantly decreased, and the difference in the nucleating activity between ABP135$_{G1-G3}$ and ABP29 was minor in the presence of low levels of $Ca^{2+}$. These results suggest that the G3 domain regulates the actin nucleating activities of ABP135$_{G1-G3}$ and ABP29 in the presence of different concentrations of $Ca^{2+}$.

## The capping effect of ABP29 is stronger than that of ABP135$_{G1-G3}$ in the presence of low $Ca^{2+}$

We examined the effects of ABP29 and ABP135$_{G1-G3}$ on the critical concentration (Cc) of actin to determine whether either of these proteins caps the barbed ends. As shown in S1A Fig, the
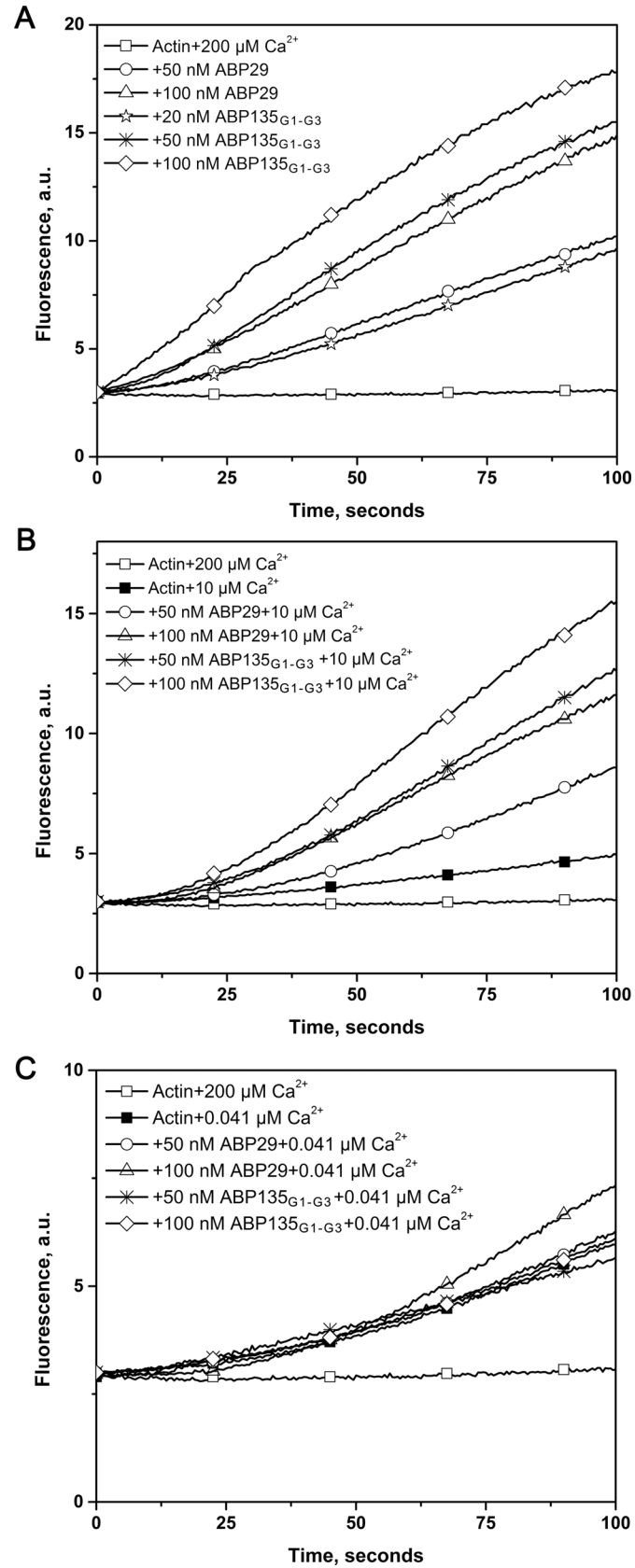
**Fig 4. Recombinant ABP29 and ABP135$_{G1-G3}$ nucleate actin polymerization.** (A) Time course of the change in pyrene fluorescence accompanying actin polymerization in the presence of ABP29 or ABP135$_{G1-G3}$. Increasing amounts of ABP29 or ABP135$_{G1-G3}$ were added to 5 µM G-actin (5% pyrene-labeled) in the presence of 200 µM free Ca$^{2+}$. Different combinations of reactions are indicated in the upper left. (B) and (C) In the presence of 10 µM free Ca$^{2+}$ and 0.041 µM free Ca$^{2+}$ respectively, time course of the change in pyrene fluorescence accompanying actin polymerization in the presence of ABP29 or ABP135$_{G1-G3}$. Different combinations of reactions are indicated in the upper left.

doi:10.1371/journal.pone.0143174.g004

Cc was shifted in the presence of ABP29 or ABP135$_{G1-G3}$, and quantitative analyses demonstrated that ABP29 increased the Cc from 0.23 ± 0.03 µM for actin filaments with free barbed ends to 0.37 ± 0.01 µM, while ABP135$_{G1-G3}$ shifted the Cc to 0.72± 0.02 µM. This shift may have resulted from G-actin binding. Then, the barbed ends of actin filaments were capped with CapG, and ABP29 was found to increase the Cc of actin filaments from 0.51 ± 0.03 µM to 0.69 ± 0.01 µM, while ABP135$_{G1-G3}$ shifted the Cc to 0.85± 0.02 µM. These results (S1B Fig) indicate that both ABP29 and ABP135$_{G1-G3}$ could bind G-actin. Seed elongation assays were subsequently performed to examine whether ABP29 and ABP135$_{G1-G3}$ exhibit similar activities in inhibiting actin elongation from the barbed ends. As shown in Fig 5A, ABP29 and ABP135$_{G1-G3}$ could suppress F-actin elongation effectively in the presence of high concentrations of free Ca$^{2+}$ (200 µM and 10 µM). However, when free Ca$^{2+}$ was chelated by EGTA to 0.041 µM, the capping activity of ABP135$_{G1-G3}$ was arrested more dramatically than ABP29, and ABP29 had a stronger inhibitory effect on actin elongation than ABP135$_{G1-G3}$ (Fig 5B and 5C). Taken together, these data suggest that the inhibitory effects of ABP135$_{G1-G3}$ are more sensitive to Ca$^{2+}$ than those of ABP29 due to its extra G3 domain relative to ABP29 and that the capping activity of ABP29 is stronger than that of ABP135$_{G1-G3}$ in the presence of low Ca$^{2+}$ concentrations.

## ABP29 inhibits F-actin depolymerization, whereas ABP135$_{G1-G3}$ accelerates its depolymerization during the process of dilution-mediated depolymerization

Recent studies have demonstrated that ABP29 inhibits F-actin depolymerization in a dilution-mediated actin depolymerization assay [20], whereas LdABP41 promotes actin depolymerization [30]. However, it is not clear whether these differences are caused by the G3 domain because the coding gene for LdABP41 is unknown [19]. Therefore, the same assay was performed to verify the function of the G3 domain in actin dynamics. The results showed that ABP29 stabilized F-actin by inhibiting actin depolymerization in a Ca$^{2+}$-dependent manner during the process of dilution-mediated depolymerization, as indicated by previous studies [20] (Fig 6A–6C), whereas ABP135$_{G1-G3}$ accelerated F-actin depolymerization in a manner similar to LdABP41, except that LdABP41 possesses higher activity [30]. In addition, as shown in Fig 6B and 6C, the process of depolymerization by ABP135$_{G1-G3}$ can be divided into two phases, similar to the function of G1-G3 domains of gelsolin [42]. During the early phase, ABP135$_{G1-G3}$ may sever actin filaments to generate greater numbers of filament ends and accelerate F-actin depolymerization in a Ca$^{2+}$-sensitive manner. All of the results described above demonstrate that the G3 domain plays a vital role in regulating ABP135$_{G1-G3}$ relative to ABP29 during the process of dilution-mediated depolymerization.

Recent studies have also shown that ABP29 and LdABP41, mRNA-spliced variants of lily ABP135, are expressed in pollen tubes [19,20]. Thus, these proteins may compete in the regulation of actin dynamics. To determine whether and how ABP29 affects ABP135$_{G1-G3}$ activity and vice versa, actin depolymerization assays were conducted. As shown in Fig 7A, when the amount of ABP135$_{G1-G3}$ was fixed (at 1000 nM) and the concentration of ABP29 was varied (0
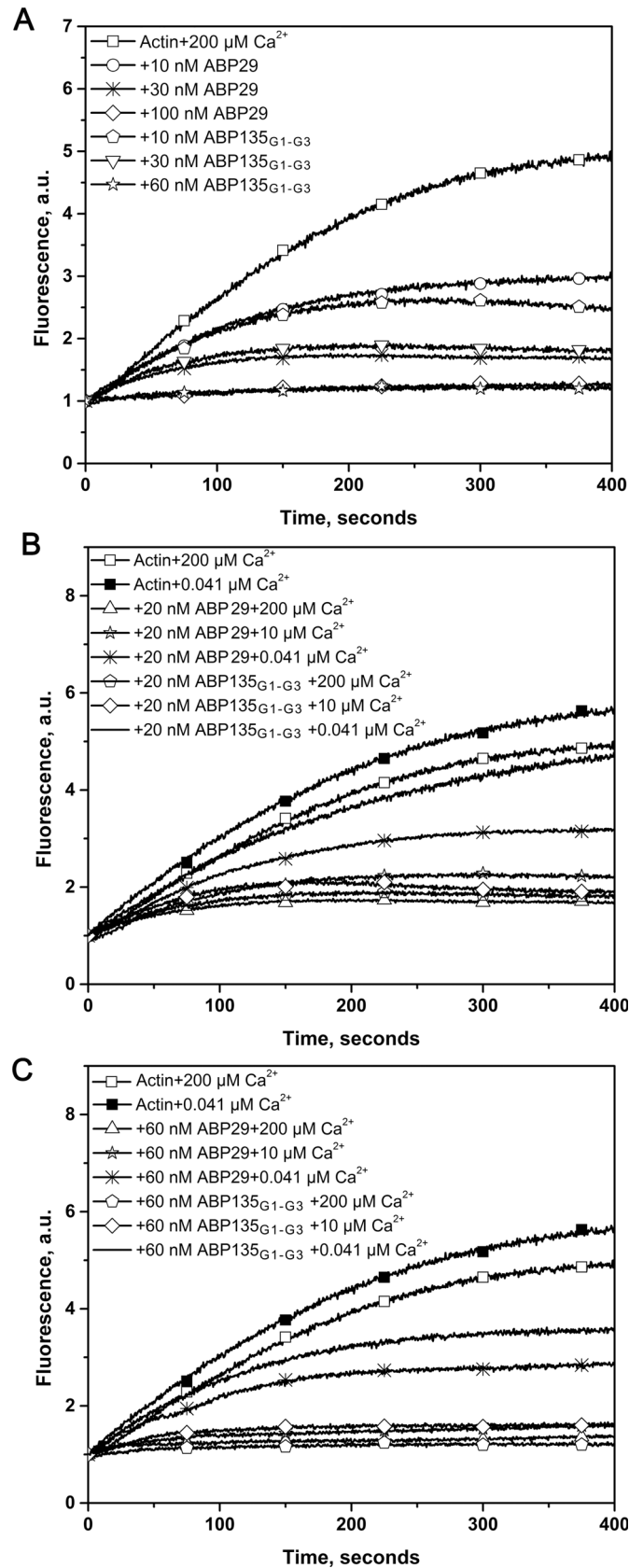
**Fig 5. Recombinant ABP29 and ABP135$_{G1-G3}$ inhibit actin filament elongation.** (A) Kinetics of actin filament barbed end elongation with various concentrations of ABP29 or ABP135$_{G1-G3}$ in the presence of 200 μM free Ca$^{2+}$. Different combinations of reactions are indicated in the upper left. (B) and (C) Kinetics of actin filament barbed end elongation with 20 nM and 60 nM ABP29 or ABP135$_{G1-G3}$, respectively, in the presence of different concentrations of free Ca$^{2+}$. Different combinations of reactions are indicated in the upper left.

doi:10.1371/journal.pone.0143174.g005

nM, -200 nM or -300 nM), ABP29 reduced the effects of ABP135$_{G1-G3}$ on F-actin depolymerization. Similarly, when the amount of ABP29 was fixed (at 300 nM) and the concentration of ABP135$_{G1-G3}$ was varied (0 nM, -1000 nM or -2000 nM), ABP135$_{G1-G3}$ effectively reduced the effects of ABP29. Taken together, the presence or deletion of the G3 domain may play a special cooperative role in regulating dynamic actin remodeling in plants.

## ABP29 stabilizes actin by inhibiting F-actin depolymerization during the process of dilution-mediated depolymerization in contrast with typical villin/gelsolin/fragmin superfamily members

Interestingly, ABP29, which contains the G1 and G2 domains and parts of the G2-G3 linkers of ABP135, inhibits F-actin depolymerization in a Ca$^{2+}$-dependent manner [20]. To elucidate the underlying difference and determine whether the G1-G2 domains of ABP29 alone can enhance actin filament depolymerization, we generated two truncated variants of ABP29. The first was ABP29-△C6, a version of ABP29 in which six C-terminal amino acids of ABP29 were removed (this six amino acid sequence is not included in ABP135). The second was ABP29$_{G1-G2}$, which included only the G1 and G2 domains of ABP29 (Fig 1B). As shown in Fig 8, ABP29-△C6 and ABP29$_{G1-G2}$ severed and/or depolymerized actin filaments, and during the process of dilution-mediated depolymerization, they inhibited F-actin depolymerization in a Ca$^{2+}$-sensitive manner similar to ABP29. We found that the effect exerted by ABP29 on actin depolymerization was the opposite of that of typical villin/gelsolin/fragmin superfamily members, which instead accelerate F-actin depolymerization during the process of dilution-mediated depolymerization.

## Discussion

Pollen tube growth is a vital process in angiosperms and is necessary for double fertilization. Genetic and pharmacological evidence has demonstrated that the actin cytoskeleton plays a vital role in this process; the disruption of actin filaments leads to the retardation of pollen germination and pollen tube growth [20,43–48]. In addition, Ca$^{2+}$ has been shown to exist in the pollen tube in a concentration gradient and to be indispensable for this process [49,50]. For example, within the pollen tube, the Ca$^{2+}$ concentration is 5–10 μM in the tip area but 200 nM in the shank [39–41,49,50]. Actin cytoskeleton dynamics are fundamental to the role of the cytoskeleton in pollen tube growth, which is directly regulated by numerous ABPs [18,51]. Among them, the villin/gelsolin/fragmin superfamily is a major group of Ca$^{2+}$-dependent ABPs and may act as the "sensor" and "executor" of the Ca$^{2+}$ [13,19,30]. Importantly, many members of this family have been identified in pollen and have been shown to be necessary for pollen germination and pollen tube growth, regulating diverse actin structures in various stages and spaces, such as AtVLN5 [38] and AtVLN2 [52] in *Arabidopsis thaliana*, ABP135 [14,15] and ABP115 [16,17] in *Lilium longiflorum*, PrABP80 in *Papaver rhoeas* [13], LdABP41 in *Lilium davidii* [19] and ABP29 in *Lilium longiflorum* [20]. The functions of the proteins in this superfamily are determined by different gelsolin-like domains, which play distinct roles in actin dynamics [1,3,5]. To date, the function of the G3 domain remains unclear. Therefore,
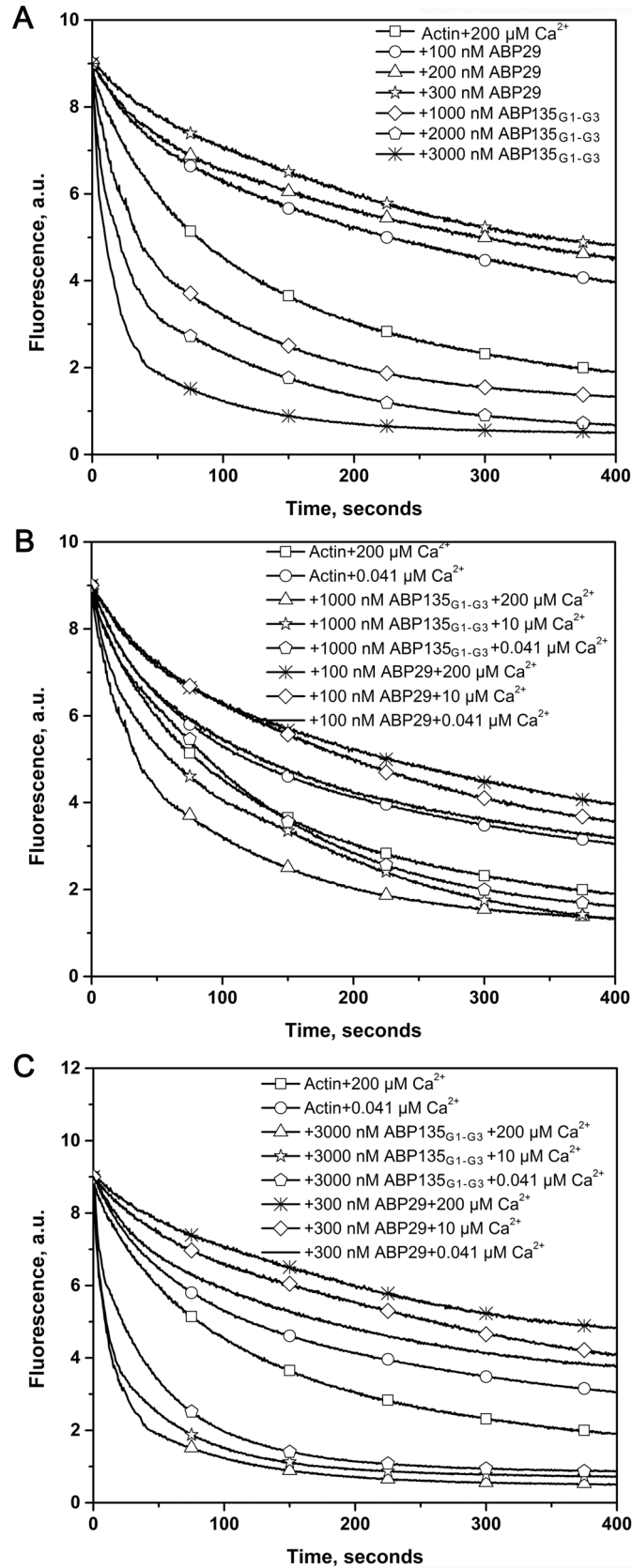
**Fig 6. Recombinant ABP29 and ABP135$_{G1-G3}$ exert opposing effects on the actin dynamics of depolymerization.** (A) Kinetics of actin depolymerization in the presence of various concentrations of ABP29 or ABP135$_{G1-G3}$ in the presence of 200 μM free Ca$^{2+}$. The change in pyrene fluorescence accompanying actin depolymerization was monitored. Different combinations of reactions are indicated in the upper right. (B) and (C) Fixed concentrations of ABP29 or ABP135$_{G1-G3}$ were incubated with 5 μM F-actin (50% pyrene-labeled) in the presence of free Ca$^{2+}$ chelated by EGTA. The change in pyrene fluorescence accompanying actin depolymerization was monitored. Different combinations of reactions are indicated in the upper right.

elucidating the function of this domain would contribute to our understanding of the mechanism by which members of the villin/gelsolin/fragmin superfamily regulate actin dynamics in pollen. In this paper, we compared differences between ABP29 and ABP135$_{G1-G3}$ in terms of actin dynamics in the presence of different concentrations of Ca$^{2+}$. The results demonstrated that ABP135$_{G1-G3}$ had greater severing and/or depolymerization and nucleating abilities than ABP29 in the presence of high levels of Ca$^{2+}$ (200 and 10 μM) (Figs 1C and 1D, 2 and 3), whereas ABP29 exhibited greater capping activity relative to ABP135$_{G1-G3}$ in the presence of low concentrations of Ca$^{2+}$. These findings may also indicate that ABP29 experiences slower off rates and therefore remains bound to the filament barbed ends to protect them from both depolymerization and elongation. Moreover, ABP29 inhibits F-actin depolymerization in a Ca$^{2+}$-dependent manner during the process of dilution-mediated depolymerization (Fig 6). All of these results suggest that the G3 domain plays a specific role in regulating the activities of villin/gelsolin/fragmin superfamily members in the presence of different Ca$^{2+}$ concentrations.

What is puzzling is that the severing and/or depolymerization activity of ABP135$_{G1-G3}$, which contains the G3 domain, is stronger than that of ABP29 in the presence of high concentrations of Ca$^{2+}$ (such as 200 μM and 10 μM). Although the crystal structures of ABP135$_{G1-G3}$ and ABP29 have not been determined, the structures of full-length gelsolin [5], the G1-G3 domains of gelsolin in complex with G-actin [53,29] and the G4-G6/actin complex [54] and 3D structure of villin [55] have been solved. These excellent prior studies allow us to propose a model to explain the differences in actin severing and/or depolymerization abilities between ABP29 and ABP135$_{G1-G3}$ which reveals that both proteins possess highly conserved gelsolin domains [19,20,56]. The work of Peddada N. and colleagues showed that G1-G2 of gelsolin appears to prefer a collapsed state under Ca$^{2+}$-free conditions and changes to an open shape in 1 mM Ca$^{2+}$, while G1-G3 of gelsolin adopts an open three-lobed and a closed shape under Ca$^{2+}$-free and 1 mM Ca$^{2+}$ conditions, and G1-G3 with mutations in the g2-g3 linker assumes open shape under 1 mM Ca$^{2+}$ conditions [42]. It may be that ABP135$_{G1-G3}$ is a same shape as mutations of G1-G3 of gelsolin. As shown in S2B Fig, in the absence of Ca$^{2+}$, ABP135$_{G1-G3}$ is compact and inactive. According to the work of Burtnick L. D. and coworkers [53,57] as well as the molecular model of ABP135$_{G1-G3}$, the severing steps consist of the following activities: when there are high concentrations of Ca$^{2+}$ (10 μM Ca$^{2+}$), Ca$^{2+}$ binding to the G3 domain of ABP135$_{G1-G3}$ weakens and opens the G1-G3 latch and straightens its long helix. Then, Ca$^{2+}$ binding to the G2 domain further drives the G2–G3 domains towards an active conformation, exposing the buried F-actin binding site in the G2 domain. Finally, the G2 domain binds to the side of the F-actin, and the G1 domain wedges two adjacent actins in the longitudinal axis, causing a cleavage and then leading the G1 domain to bind to the barbed ends simultaneously, resulting in severing. Similarly, although lacking the G3 domain, Ca$^{2+}$ binding to the G2 domain can drive the G1-G2 domains toward a fully active conformation. Then, like ABP135$_{G1-G3}$, the G2 domain binds to the side of F-actin, and the G1 domain wedges two adjacent actins into the longitudinal axis, resulting in severing (S2A Fig). As shown in S2B Fig, in the presence of Ca$^{2+}$, the G2 domain binds to the actin subdomain 2, and the G3 domain may also bind to the actin subdomain 1, which may stabilize the binding activity between the G2
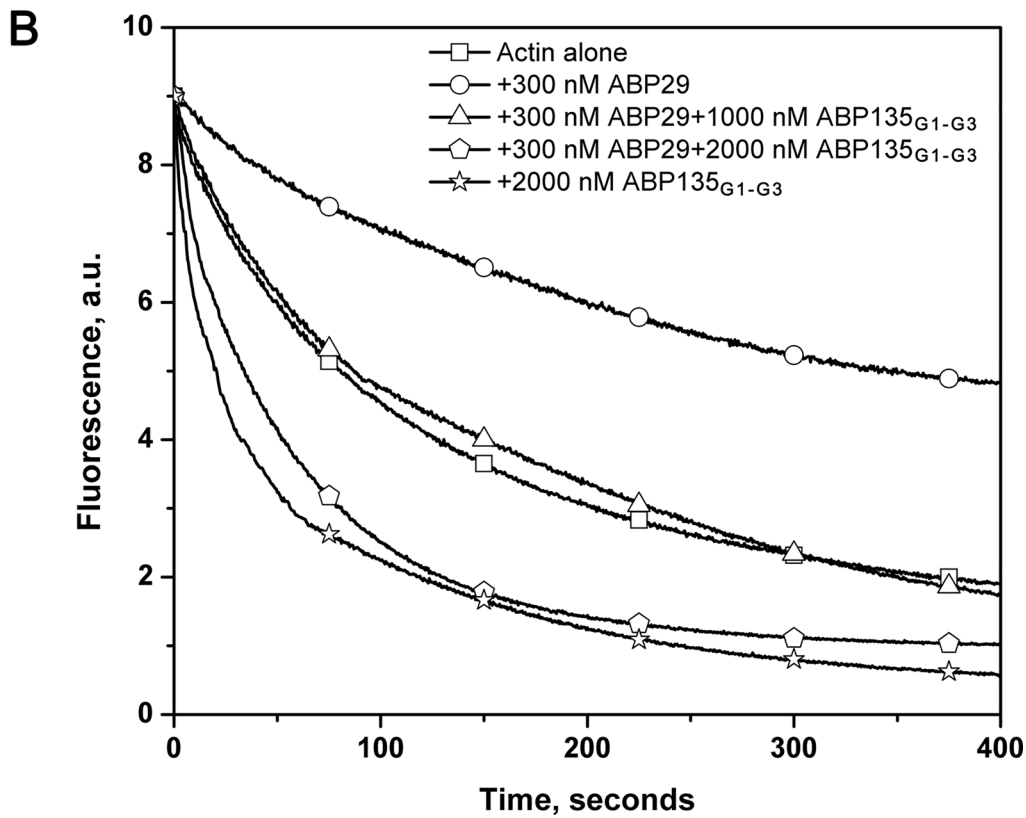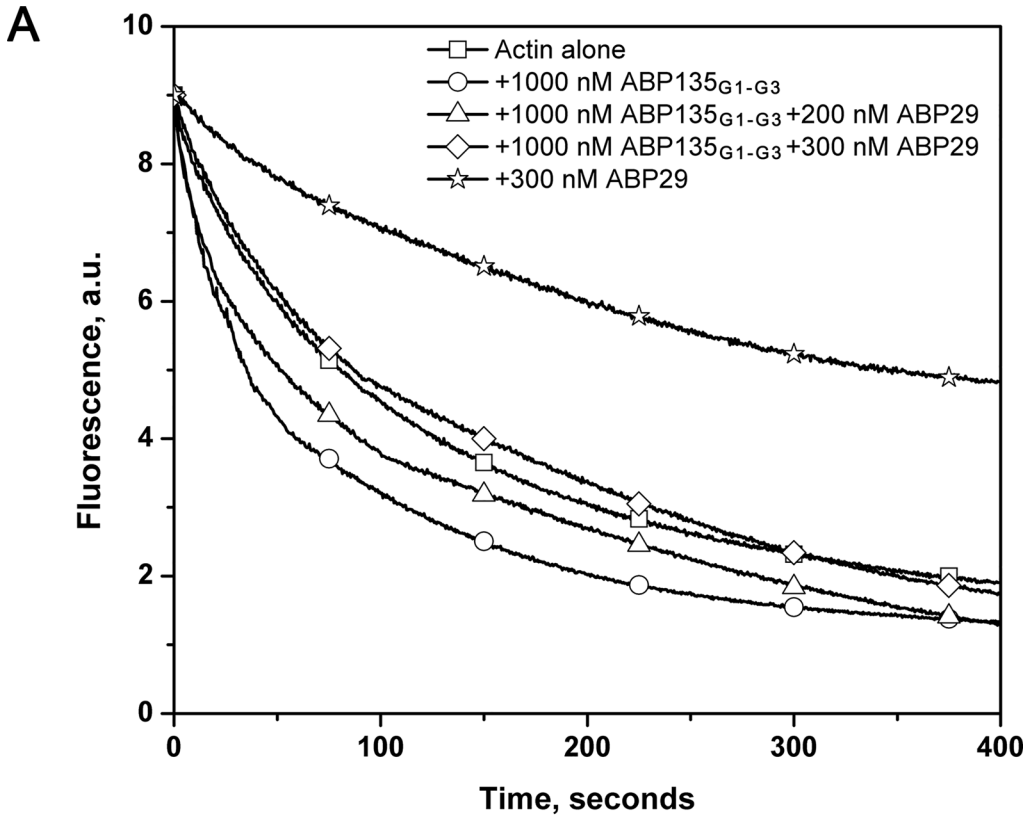
A



B

**Fig 7. ABP29 and ABP135$_{G1-G3}$ compete with each other in actin depolymerization.** (A) Competition experiments between ABP29 and ABP135$_{G1-G3}$ were performed during the F-actin depolymerization process. A fixed amount of ABP135$_{G1-G3}$ (1000 nM) and different amounts of ABP29 (0, 200 nM and 300 nM) were simultaneously incubated with 5 μM F-actin (50% pyrene-labeled). The kinetics of actin depolymerization were monitored by measuring the decrease in pyrene fluorescence intensity. Different combinations of reactions are indicated in the upper right. (B) A fixed amount of ABP29 (300 nM) and different amounts of ABP135$_{G1-G3}$ (0, 1000 nM and 2000 nM) were simultaneously incubated with 5 μM F-actin (50% pyrene-labeled). Different combinations of reactions are indicated in the upper right.

domain and the actin. Because it lacks the G3 domain, the actin severing and/or depolymerization activity of ABP29 is weaker than that of ABP135$_{G1-G3}$. We proposed that the G3 domain may partially contribute to actin severing activity by stabilizing the binding activity between the G2 domain and actin. Furthermore, Selden et al. [58] have proposed that the G1-G3 domains cooperatively sever F-actin. Therefore, ABP135$_{G1-G3}$ may lead to a cooperative severing of F-actin by using two molecules that bind F-actin in close proximity, thereby increasing the severing efficiency.

In general, the villin/gelsolin/fragmin superfamily proteins sever F-actin and then generate more actin ends, thereby accelerating actin depolymerization, as demonstrated by dilution-mediated actin depolymerization assay [1]; however, a capping protein binds to the F-actin ends and thus inhibits actin depolymerization [59]. *In vitro*, ABP135$_{G1-G3}$ and ABP29 exhibit actin severing and/or depolymerization and capping activities; however, ABP29 inhibits F-actin depolymerization, whereas ABP135$_{G1-G3}$ accelerates its depolymerization during the process of dilution-mediated depolymerization. We propose that ABP135$_{G1-G3}$ might preferentially bind to F-actin because the G3 domain stabilizes the interaction between the G2 domain and the F-actin. Otherwise, the capping activity of ABP29 plays a main effect on F-actin for the special structure of ABP29 with G1-G2 domains. Without the latch of the G3 domain, the G1 domain of ABP29 could directly bind to the ends of F-actin, leading to cap the barbed ends after the severing. So ABP29 resulted in more actin in the supernatants and shorter filaments compared to ABP135$_{G1-G3}$ (Figs 1 and 2) and stabilized F-actin during dilution-mediated depolymerization. To the best of our knowledge, thus far, ABP29 is a natural product and the only member of the villin/gelsolin/fragmin superfamily with severing and capping activities that stabilizes F-actin during dilution-mediated depolymerization in a Ca$^{2+}$-dependent manner. We thus obtained two truncated versions of ABP29: ABP29-△C6 and ABP29$_{G1-2}$. As shown in Fig 8, like ABP29 (Fig 1), ABP29-△C6 and ABP29$_{G1-G2}$ sever and/or depolymerize actin filaments and protect F-actin from dilution-mediated depolymerization (Fig 8A and 8B). Because native ABP29 existing in pollen only contains the G1-G2 domains, we speculate that plants may have evolved a special mechanism by which they fulfill specific roles in regulating actin dynamics during this process. Therefore, it would be interesting and helpful to conduct further structural and biochemical analyses of the G1-G2 domains to explore this potential mechanism in plants.

The biochemical activities and expression patterns of the villin/gelsolin/fragmin superfamily members are diverse and distinct during pollen germination and pollen tube growth [30]. For example, in ungerminated lily pollen, only PrABP80, LdABP41 and ABP29 can be found, indicating that these proteins play vital roles in maintaining the actin cytoskeleton in a dot-like form as a storage stage via their actin severing, nucleating and capping activities [30]. After pollen germination, the expression levels of LdABP41 decrease dramatically, and ABP135 and ABP115 specifically emerge [30]. ABP135 and ABP115 may participate in the formation of higher-order actin bundles via their actin severing, bundling, nucleating and capping activities. The expression levels of ABP29 remain stable throughout the process, indicating that it consistently regulates actin dynamics [30]. In this study, we used rabbit muscle actin and lily proteins to perform the experiments because actin is one of the most highly conserved proteins, as it has
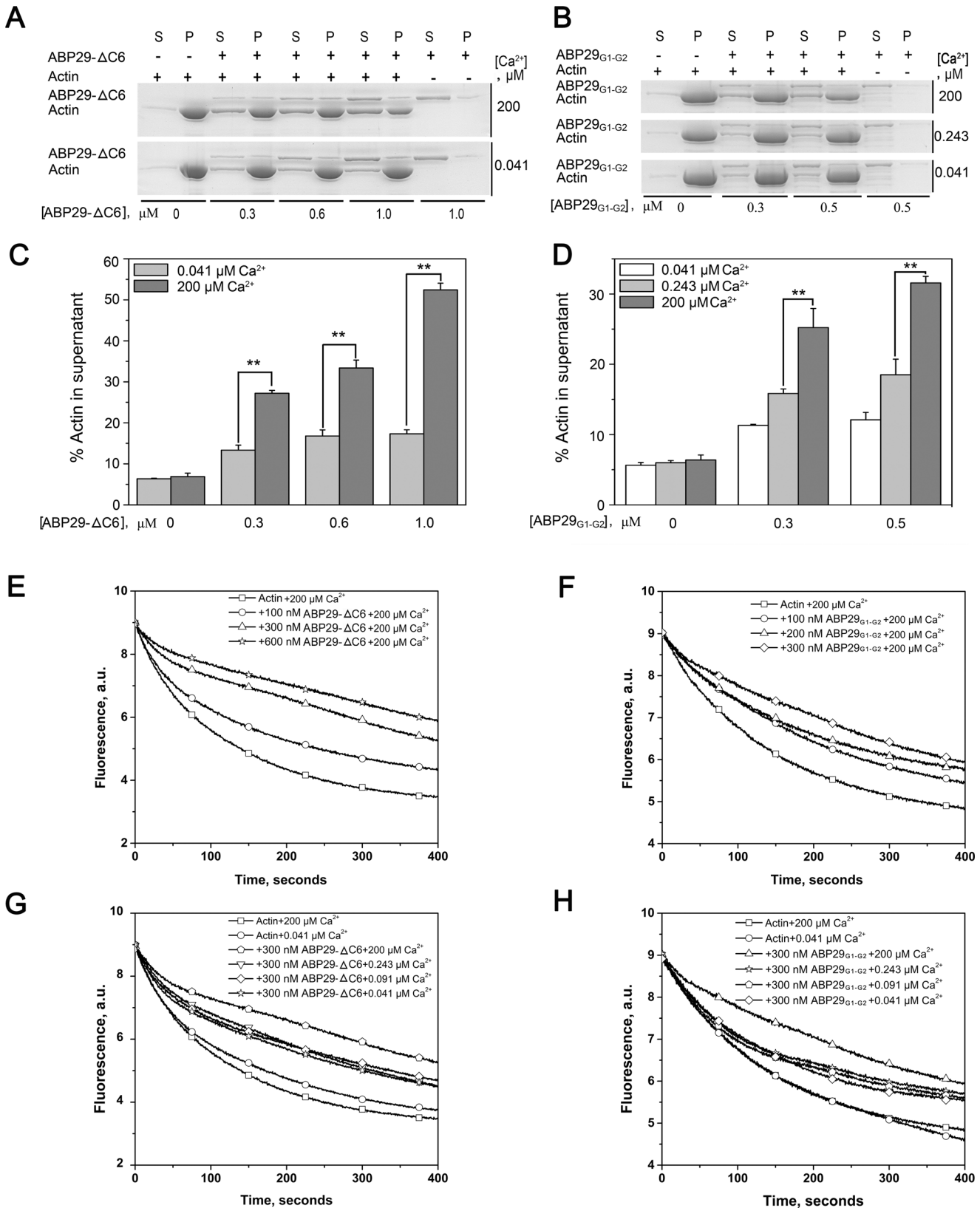
Fig 8. Recombinant ABP29-△C6 and ABP29$_{G1-G2}$ sever and/or depolymerize F-actin and stabilize F-actin *in vitro*. (A) The severing and/or depolymerization activity of ABP29-△C6 exerted on actin filaments was determined using high-speed co-sedimentation assays in the presence of 200 μM

and 0.041 μM free $Ca^{2+}$; "(s)" indicates supernatant, and "(p)" indicates pellets. (B) The severing and/or depolymerization activity of $ABP29_{G1-G2}$ exerted on actin filaments was determined using high-speed co-sedimentation assays in the presence of various concentrations of free $Ca^{2+}$ (200, 0.243 and 0.041 μM); "(s)" indicates supernatant, and "(p)" indicates pellets. (C) and (E) Statistical analysis results from (A) and (B), respectively. The error bars represent ± SE (n = 3); **P < 0.01 (Student's $t$ test). (E) and (F) Kinetics of actin depolymerization in the presence of various concentrations of $ABP29_{G1-G2}$ and ABP29-△C6 in the presence of 200 μM free $Ca^{2+}$. The change in pyrene fluorescence accompanying actin depolymerization was monitored. Different combinations of the reactions are indicated in the upper right. (G) and (H) 300 nM $ABP29_{G1-G2}$ or ABP29-△C6, respectively, was incubated with 5 μM F-actin (50% pyrene-labeled) for 5 min in the presence of various concentrations of free $Ca^{2+}$ chelated by EGTA. The kinetics of actin depolymerization were monitored by measuring the change in fluorescence intensity. Different combinations of reactions are indicated in the upper right.

doi:10.1371/journal.pone.0143174.g008

changed little over the course of evolution [60]. We showed that $ABP135_{G1-G3}$ and ABP29 possess similar actions in terms of actin severing and/or depolymerization, nucleating and capping, but their activities exhibit some differences under different concentrations of $Ca^{2+}$. Moreover, these proteins neutralize activity in the dilution-mediated depolymerization assay, and this difference is specifically attributable to the G3 domain. In conclusion, the presence or absence of the G3 domain may be an important evolutionary mechanism to regulate the activities of gelsolin/fragmin/fragmin proteins, which is necessary for pollen germination and pollen tube growth.

## Supporting Information

**S1 Fig. ABP29 and ABP135G1-G3 shifted the critical concentration of actin assembly.** Pyrene-labeled G-actin (20% labeled) with varying concentrations (0–4 μM) was polymerized alone or with a 1/200 molar ratio of human CapG:actin for 18 h at room temperature in the presence of 0.5 μM ABP29 or $ABP135_{G1-G3}$ in F-buffer, and the final fluorescence intensity of pyrene (excitation at 365nm and emission at 407 nm) was measured.(A) Actin polymerized alone in the presence of 0.5 μM ABP29 or $ABP135_{G1-G3}$ in F-buffer; (B) actin polymerized with a 1/200 molar ratio of human CapG:actin in the presence of 0.5 μM ABP29 or $ABP135_{G1-G3}$ in F-buffer. Linear best fit of the data, and plotted as arbitrary fluorescence units versus actin concentration, was used to determine the intercept with x axis.
(TIF)

**S2 Fig. The models of ABP29:actin and $ABP135_{G1-G3}$:actin.** (A) Model of $Ca^{2+}$-free ABP29 interacting with actin: ABP29 contains the G1 and G2 domains. Actin is colored in gray, with subdomains 1, 2, 3 and 4 indicated. $Ca^{2+}$ ions are depicted as green spheres. (B) Model of $Ca^{2+}$-free $ABP135_{G1-G3}$ interacting with actin. (C) and (D) Models of the active states of ABP29:actin and $ABP135_{G1-G3}$:actin, respectively. Molecular graphics were created with VMD software package. Crystal structure of $Ca^{2+}$-free plasma gelsolin (PDB:1D0N); crystal structures of gelsolin domains G1-G3:actin (PDB:1RGI) and the gelsolin G4-G6/ACTIN complex (PDB:1H1V).
(TIF)

## Acknowledgments

## Author Contributions

Conceived and designed the experiments: YX DQ LA. Performed the experiments: DQ QN YY HL YZ JZ QB PZ. Analyzed the data: DQ LA YX. Wrote the paper: DQ YX.

# References

1. Sun H, Yamamoto M, Mejillano M, Yin HL (1999) Gelsolin, a multifunctional actin regulatory protein. J Biol Chem 274: 33179–33182. PMID: 10559185

2. Silacci P, Mazzolai L, Gauci C, Stergiopulos N, Yin HL, Hayozb D (2004) Gelsolin superfamily proteins: Key regulation of cellular functions. Cell Mol Life Sci 61: 2614–2623. PMID: 15526166

3. Mcgough AM, Staiger CJ, Min JK, Simonetti KD (2003) The gelsolin family of actin regulatory proteins: Modular structures, versatile functions. FEBS Letters 552: 75–81. PMID: 14527663

4. Kwiatkowski DJ, Stossel TP, Orkin SH, Mole JE, Colten HR, Yin HL (1986) Plasma and cytoplasmic gelsolins are encoded by a single gene and contain a duplicated actin-binding domain. Nature 323: 455–458. PMID: 3020431

5. Burtnick LD, Koepf EK, Grimes J, Jones EY, Stuart DI, McLaughlin PJ, et al. (1997) The crystal structure of plasma gelsolin: Implications for actin severing, capping, and nucleation. Cell 90: 661–670. PMID: 9288746

6. Friederich E, Vancompernolle K, Louvard D, Vandekerckhove J (1999) Villin function in the organization of the actin cytoskeleton. Correlation of in vivo effects to its biochemical activities in vitro. J Biol Chem 274: 26751–60. PMID: 10480879

7. Bazari WL, Matsudaira P, Wallek M, Smeal T, Jakes R, Ahmed Y (1988) Villin sequence and peptide map identify six homologous domains. Proc Natl Acad Sci USA 85: 4986–90. PMID: 2839826

8. Pellieux C, Desgeorges A, Pigeon CH, Chambaz C, Yin HL, Hayoz D, et al. (2003) Cap G, a gelsolin family protein modulating protective effects of unidirectional shear stress. J Biol Chem 278: 29136–29144. PMID: 12754261

9. Klaavuniemi T, Yamashiro S, Ono S (2008) Caenorhabditis elegans gelsolin-like protein 1 is a novel actin filament-severing protein with four gelsolin-like repeats. J Biol Chem 283: 26071–26080. doi: 10.1074/jbc.M803618200 PMID: 18640981

10. Klahre U, Friederich E, Kost B, Louvard D, Chua NH (2000) Villin-like actin-binding proteins are expressed ubiquitously in arabidopsis. Plant Physiol 122: 35–48. PMID: 10631247

11. Mittermann I, Voronin V, Heberle-Bors E, Valenta R (2005) Identification of a villin-related tobacco protein as a novel cross-reactive plant allergen. FEBS Letters 579: 3807–3813. PMID: 15978584

12. Ghoshdastider U, Popp D, Burtnick LD, Robinson RC (2013) The expanding superfamily of gelsolin homology domain proteins. Cytoskeleton 70: 775–795. doi: 10.1002/cm.21149 PMID: 24155256

13. Huang S, Blanchoin L, Chaudhry F, Franklin-Tong VE, Staiger CJ (2004) A gelsolin-like protein from Papaver rhoeas pollen (PrABP80) stimulates calcium-regulated severing and depolymerization of actin filaments. J Biol Chem 279: 23364–23375. PMID: 15039433

14. Yokota E, Shimmen T (1999) The 135-kDa actin-bundling protein from lily pollen tubes arranges F-actin into bundles with uniform polarity. Planta 209: 264–266. PMID: 10436230

15. Vidali L, Yokota E, Cheung AY, Shimmen T, Hepler PK (1999) The 135 kDa actin-bundling protein from Lilium longiflorum pollen is the plant homologue of villin. Protoplasma 209: 283–291.

16. Nakayasu T, Yokota E, Shimmen T (1998) Purification of an actin-binding protein composed of 115-kDa polypeptide from pollen tubes of lily. Biochem Biophys Res Commun 249: 61–65. PMID: 9705832

17. Yokota E, Vidali L, Tominaga M, Tahara H, Orii H, Morizane Y, et al. (2003) Plant 115-kDa actin-filament bundling protein, P-115-ABP, is a homolog of plant villin and widely distributed in cells. Plant Cell Physiol I44: 1088–1099.

18. Staiger CJ, Hussey PJ (2004) Actin and actin-modulating proteins: In The plant cytoskeleton in cell differentiation and development (Hussey PJ eds.). Blackwell, UK. Press. 32p.

19. Fan X, Hou J, Chen X, Chaudhry F, Staiger CJ, Ren H (2004) Identification and characterization of a $Ca^{2+}$-dependent actin filament-severing protein from lily pollen. Plant Physiol 136: 3979–3989. PMID: 15557101

20. Xiang Y, Huang X, Wang T, Zhang Y, Liu Q, Hussey PJ, et al. (2007) Actin binding protein 29 from Lilium pollen plays an important role in dynamic actin remodeling. Plant Cell 19: 1930–1946. PMID: 17586658

21. Su H, Wang T, Dong H, Ren H (2007) The villin/gelsolin/fragmin superfamily proteins in plants. J Integr Plant Biol 48: 1183–1191.

22. Yin HL, Iida K, Janmey PA (1988) Identification of a polyphosphoinositide-modulated domain in gelsolin which binds to the sides of actin filaments. J Cell Biol 106: 805–812. PMID: 2831234

23. Kwiatkowski DJ, Janmey PA, Yin HL (1989) Identification of critical functional and regulatory domains in gelsolin. J Cell Biol 108: 1717–1726. PMID: 2541138

24.  Sun H, Wooten DC, Janmey PA, Yin HL (1994) The actin side-binding domain of gelsolin also caps actin-filaments. Implications for actin filament severing. J Biol Chem 269: 9473–9479. PMID: 8144531

25.  Maciver SK, Ternent D, Mclaughlin PJ (2000) Domain 2 of gelsolin binds directly to tropomyosin. FEBS letters 473: 71–75. PMID: 10802062

26.  Liu Z, Ono S (2013) Regulatory role of the second gelsolin-like domain of Caenorhabditis elegans gelsolin-like protein 1 (GSNL-1) in its calcium-dependent conformation and actin-regulatory activities. Cytoskeleton 70: 228–239. doi: 10.1002/cm.21103 PMID: 23475707

27.  Pope BJ, Maciver S, Weeds AG (1995) Localization of the calcium-sensitive actin monomer binding site in gelsolin to segment 4 and identification of calcium-binding sites. Biochemistry 34: 1583–1588. PMID: 7849017

28.  Pope BJ, Gooch JT, Weeds AG (1997) Probing the effects of calcium on gelsolin. Biochemistry 36: 15848–15855. PMID: 9398317

29.  Nag S, Ma Q, Wang H, Chumnarnsilpa S, Lee WL, Larsson M, et al. (2009) $Ca^{2+}$ binding by domain 2 plays a critical role in the activation and stabilization of gelsolin. Proc Natl Acad Sci USA 106: 13713–13718. doi: 10.1073/pnas.0812374106 PMID: 19666512

30.  Wang T, Xiang Y, Hou J, Ren H (2008) ABP41 is involved in the pollen tube development via fragmenting actin filaments. Mol Plant 1: 1048–1055. doi: 10.1093/mp/ssn073 PMID: 19825602

31.  Ma B, Qian D, Nan Q, Tan C, An L, Xiang Y (2012) Arabidopsis V-ATPase B subunits are involved in actin cytoskeleton remodeling via binding to, bundling and stabilizing F-actin. J Biol Chem 287: 19008–19017. doi: 10.1074/jbc.M111.281873 PMID: 22371505

32.  Pardee JD, Spudich JA (1982) Purification of muscle actin. Methods Cell Biol 24: 271–289. PMID: 7098993

33.  Pollard TD (1984) Polymerization of ADP-actin. J Cell Biol 99: 769–777. PMID: 6540783

34.  Yarmola EG, Somasundaram T, Boring TA, Spector I, Bubb MR (2000) Actin-latrunculin A structure and function. Differential modulation of actin-binding protein function by latrunculin A. J Biol Chem 275: 28120–28127. PMID: 10859320

35.  Khurana P, Henty JL, Huang S, Staiger AM, Blanchoin L, Staiger CJ (2010) Arabidopsis VILLIN1 and VILLIN3 have over-lapping and distinct activities in actin bundle formation and turnover. Plant Cell 22: 2727–2748. doi: 10.1105/tpc.110.076240 PMID: 20807878

36.  Liu Z, Kanzawa N, Ono S (2011) Calcium-sensitive activity and conformation of Caenorhabditis elegans gelsolin-like protein 1 are altered by mutations in the first gelsolin-like domain. J Biol Chem 286: 34051–34059. doi: 10.1074/jbc.M111.237404 PMID: 21840993

37.  Zhang Y, Vorobiev SM, Gibson BG, Hao B, Sidhu GS, Mishra VS, et al. (2013) A CapG gain-of-function mutant reveals critical structural and functional determinants for actin filament severing. EMBO J 25: 4458–4467.

38.  Zhang H, Qu X, Bao C, Khurana P, Wang Q, Xie Y, et al. (2010) Arabidopsis VILLIN5, an actin filament bundling and severing protein, is necessary for normal pollen tube growth. Plant Cell 22: 2749–2767. doi: 10.1105/tpc.110.076257 PMID: 20807879

39.  Holdaway-Clarke TL, Hepler PK (2003) Control of pollen tube growth: role of ion gradients and fluxes. New Phytologist 159: 539–563.

40.  Kroeger JH, Geitmann A, Grant M (2008) Model for calcium dependent oscillatory growth in pollen tubes. J Theor Biol 253: 363–374. doi: 10.1016/j.jtbi.2008.02.042 PMID: 18471831

41.  Messerli MA, Creton R, Jaffe LF, Robinson KR (2000) Periodic increases in elongation rate precede increases in cytosolic $Ca^{2+}$ during pollen tube growth. Dev Biol 222: 84–98. PMID: 10885748

42.  Peddada N, Sagar A, Rathore YS, Choudhary V, Pattnaik UBK, Khatri N, et al. (2013) Global shapes of F-actin depolymerization-competent minimal gelsolins insight into the role of g2-g3 linker in PH/$Ca^{2+}$ insensitivity of the first half. J Biol Chem 288: 28266–28282. doi: 10.1074/jbc.M113.463224 PMID: 23940055

43.  Gibbon BC, Kovar DR, Staiger CJ (1999) Latrunculin B has different effects on pollen germination and tube growth. Plant Cell 11: 2349–2363. PMID: 10590163

44.  Vidali L, Mckenna ST, Hepler PK (2001) Actin polymerization is essential for pollen tube growth. Mol Biol Cell 12: 2534–2545. PMID: 11514633

45.  Chen C, Wong EI, Vidali L, Estavillo A, Hepler PK, Wu HM, et al. (2002) The regulation of actin organization by actin-depolymerizing factor in elongating pollen tubes. Plant Cell 14: 2175–2190. PMID: 12215514

46.  Cole RA, Fowler JE (2006) Polarized growth: Maintaining focus on the tip. Curr Opin Plant Biol 9: 579–588. PMID: 17010659

47. Jia H, Li J, Zhu J, Fan T, Qian D, Zhou Y, et al. (2013) *Arabidopsis* CROLIN1, a novel plant actin-binding protein, functions in cross-linking and stabilizing actin filaments. J Biol Chem 288: 32277–32288. doi: 10.1074/jbc.M113.483594 PMID: 24072702

48. Zheng Y, Xie Y, Jiang Y, Qu X, Huang S (2013) *Arabidopsis* actin-depolymerizing factor 7 severs actin filaments and regulates actin cable turnover to promote normal pollen tube growth. Plant Cell 25: 3405–3423. doi: 10.1105/tpc.113.117820 PMID: 24058157

49. Holdaway-Clarke TL, Feijo JA, Hackett GR, Kunkel JG, Hepler PK (1997) Pollen tube growth and the intracellular cytosolic calcium gradient oscillate in phase while extracellular calcium influx is delayed. Plant Cell 9: 1999–2010. PMID: 12237353

50. Qin T, Liu X, Li J, Sun J, Song L, Mao T (2014) *Arabidopsis* microtubule-destabilizing protein 25 functions in pollen tube growth by severing actin filaments. Plant Cell 26: 325–339. doi: 10.1105/tpc.113.119768 PMID: 24424096

51. Pollard TD, Cooper JA (2009) Actin, a central player in cell shape and movement. Science 326: 1208–1212. doi: 10.1126/science.1175862 PMID: 19965462

52. Qu X, Zhang H, Xie Y, Wang J, Chen N, Huang S (2013) *Arabidopsis* villins promote actin turnover at pollen tube tips and facilitate the construction of actin collars. Plant Cell 25: 1803–1817. doi: 10.1105/tpc.113.110940 PMID: 23715472

53. Burtnick LD, Urosev D, Irobi E, Narayan K, Robinson RC (2004) Structure of the N-terminal half of gelsolin bound to actin: Roles in severing, apoptosis and FAF. EMBO J 23: 2713–2722. PMID: 15215896

54. Kolappan S, Gooch JT, Weeds AG, McLaughlin PJ (2003) Gelsolin domains 4–6 in active, actin-free conformation identifies sites of regulatory calcium ions. J Mol Biol 329: 85–92. PMID: 12742020

55. Hampton CM, Liu J, Taylor DW, DeRosier DJ, Taylor KA (2008) The 3D structure of villin as an unusual F-actin crosslinker. Structure 16: 1882–1891. doi: 10.1016/j.str.2008.09.015 PMID: 19081064

56. Humphrey W, Dalke A, Schulten K (1996) VMD: visual molecular dynamics. J Mol Graph 14: 33–38, 27–38. PMID: 8744570

57. Wang H, Chumnarnsilpa S, Loonchanta A, Li Q, Kuan Y, Robine S, et al. (2009) Helix straightening as an activation mechanism in the gelsolin superfamily of actin regulatory proteins. J Biol Chem 284: 21265–21269. doi: 10.1074/jbc.M109.019760 PMID: 19491107

58. Selden LA, Kinosian HJ, Newman J, Lincoln B, Hurwitz C, Gershman LC, et al. (1998) Severing of F-actin by the amino-terminal half of gelsolin suggests internal cooperativity in gelsolin. Biophysical J 75: 3092–3100.

59. Huang S, Blanchoin L, Kovar DR, Staiger CJ (2003) *Arabidopsis* capping protein (AtCP) is a heterodimer that regulates assembly at the barbed ends of actin filaments. J Biol Chem 278: 44832–44842. PMID: 12947123

60. Gunning PW, Ghoshdastider U, Whitaker S, Popp D, Robinson RC (2015). The evolution of compositionally and functionally distinct actin filaments. J Cell Sci. 128(11):2009–19 doi: 10.1242/jcs.165563 PMID: 25788699